SCAN-SPECIFIC ACCELERATED MRI RECONSTRUCTION USING RECURRENT NEURAL NETWORKS IN A REGULARIZED SELF-CONSISTENT FRAMEWORK

Seyed Amir Hossein Hosseini[⋆†], *Burhaneddin Yaman*[⋆†], *Chi Zhang*[⋆†],
Kâmil Uğurbil[†], *Steen Moeller*[†] *and Mehmet Akçakaya*[⋆†]

[⋆] Electrical and Computer Engineering, University of Minnesota, Minneapolis, MN, USA
[†] Center for Magnetic Resonance Research, University of Minnesota, Minneapolis, MN, USA

ABSTRACT

Long scan duration remains a challenge for high-resolution MRI. Several accelerated imaging strategies have been proposed based on deep learning (DL) that require databases of fully-sampled images for training. However, scan-specific training is desired where individual variability is important, e.g. in free-breathing cardiac MRI, or where such datasets are not available due to scan time constraints for acquiring fully-sampled data. Building on our earlier method called Self-consistent Robust Artificial-neural-networks for k-space Interpolation (sRAKI), we propose a scan-specific DL reconstruction method based on recurrent neural networks that combines training and reconstruction phases of sRAKI. We use self-consistency among coils in k-space and regularization in arbitrary domains, as well as consistency with acquired data, in each iteration of the recurrent network. Results on knee MRI show that this method improves upon parallel imaging and compressed sensing methods.

Index Terms— Parallel imaging, compressed sensing, machine learning, deep learning, neural networks, image reconstruction.

1. INTRODUCTION

Numerous research studies have recently employed deep learning as a means for accelerated MRI reconstruction to address the issue of lengthy acquisition times [1–9]. In contrast to conventional techniques based on parallel imaging [10] or compressed sensing [11], most of these techniques require large databases of fully-sampled data to supervise learning in the training phase for an end-to-end mapping from undersampled k-space/distorted image to interpolated k-space/distortion-free image. Furthermore, training databases may not include all pathologies of interest, which may lead to risks in generalizability for future diagnosis [12]. Additionally, in some cases, fully-sampled data cannot be reliably acquired due to prohibitively long scan duration, such as whole-heart coronary MRI [13].

Among the aforementioned DL methods, robust artificial-neural-networks for k-space interpolation (RAKI) takes a scan-specific approach to training [6]. It trains convolutional neural networks (CNN) on scan-specific autocalibrating signal (ACS) data for structured undersampling patterns. RAKI has shown robustness against noise amplification particularly at higher acceleration rates and lower signal to noise ratio (SNR) regimes. We have recently extended this approach to arbitrary undersampling patterns using a technique called self-consistent RAKI (sRAKI), which enforces self-consistency among coils [14, 15]. In sRAKI, training of the neural networks and reconstruction were performed separately, which can impact both effectiveness and efficiency of reconstruction. We have addressed this issue in [16] by simultaneously performing the training and iterative reconstruction phases of sRAKI using a recurrent neural network (RNN) architecture [3, 7, 17, 18]. In this sRAKI-RNN approach, only coil self-consistency [19] and data-consistency were used during training and reconstruction. However, a regularization term in image domain may be desirable to further improve image quality.

In this study, we sought to develop an RNN-based approach for sRAKI that incorporates an image domain regularizer in addition to coil self-consistency and data-consistency. The unrolled RNN is trained end-to-end on scan-specific data. The proposed method is tested in a knee MRI dataset, and compared to conventional scan-specific self-consistency approaches based on SPIRiT and ℓ_1-SPIRiT [19].

2. MATERIALS AND METHODS

2.1. Problem Formulation

Let $\mathbf{y}$ denote the undersampled noisy data from a multi-coil MRI system with n_c coils and $\mathbf{x}$ be the corresponding full k-space data across all coils. The forward model for this system is given as:

$$\mathbf{y} = \mathbf{D}\mathbf{x} + \mathbf{n}, \tag{1}$$

where $\mathbf{D}$ is the undersampling operator and $\mathbf{n}$ is acquisition noise. We use the following objective function to estimate $\mathbf{x}$ using measurements $\mathbf{y}$:

$$\arg\min_{\mathbf{x}} \|\mathbf{y} - \mathbf{D}\mathbf{x}\|_2^2 + \lambda\|\mathbf{x} - \mathbf{G}(\mathbf{x})\|_2^2 + \mathcal{R}(\mathbf{E}^H\mathbf{x}), \tag{2}$$

where $\mathbf{G}(\cdot)$ is the self-consistency interpolation function and $\mathcal{R}(\cdot)$ is the regularizer term to be trained, while $\mathbf{E}^H$ generates a SENSE-1 combined image from k-space [10]. The interpolation function $\mathbf{G}(\cdot)$ is implemented via scan-specific CNNs, which has shown to improve noise performance compared to its linear counterpart [14].

This objective function can be solved using an iterative optimization procedure. We unroll this iterative algorithm using a variable-splitting strategy [20] with quadratic penalty. First the objective function in (2) is recast as:

$$\arg\min_{\mathbf{x},\mathbf{u},\mathbf{z}} \|\mathbf{y}-\mathbf{D}\mathbf{x}\|_2^2 + \lambda\|\mathbf{u}-\mathbf{G}(\mathbf{u})\|_2^2 + \mathcal{R}(\mathbf{E}^H\mathbf{z}) + \beta_1\|\mathbf{x}-\mathbf{u}\|_2^2 + \beta_2\|\mathbf{x}-\mathbf{z}\|_2^2, \tag{3}$$

where β_1 and β_2 are parameters of the quadratic terms. This can be optimized by alternating minimization over each variable. For the i^{th} iteration, this is performed as follows:

$$\mathbf{u}^{(i)} = \arg\min_{\mathbf{u}} \lambda\|\mathbf{u}-\mathbf{G}(\mathbf{u})\|_2^2 + \beta_1\|\mathbf{x}^{(i-1)}-\mathbf{u}\|_2^2 \tag{4a}$$

$$\mathbf{z}^{(i)} = \arg\min_{\mathbf{z}} \mathcal{R}(\mathbf{E}^H\mathbf{z}) + \beta_2\|\mathbf{x}^{(i-1)}-\mathbf{z}\|_2^2, \tag{4b}$$

$$\mathbf{x}^{(i)} = \arg\min_{\mathbf{x}} \|\mathbf{y}-\mathbf{D}\mathbf{x}\|_2^2 + \beta_1\|\mathbf{x}-\mathbf{u}^{(i)}\|_2^2 + \beta_2\|\mathbf{x}-\mathbf{z}^{(i)}\|_2^2, \tag{4c}$$

where $x^{(0)}$ is the initial k-space data zero-filled for non-acquired elements. This procedure can now be unrolled for a fixed number of T iterations into an RNN as shown in **Fig. 1**. In this architecture, sub-problems (4a) and (4b) are solved via two distinct trainable CNNs, eliminating the need for parameter optimization. Furthermore, the linear sub-problem in (4c) has a closed form solution:

$$\mathbf{x}^{(i)} = (\mathbf{D}^T\mathbf{D}+(\beta_1+\beta_2)\mathbf{I})^{-1}(\mathbf{D}^T\mathbf{y}+\beta_1\mathbf{u}^{(i)}+\beta_2\mathbf{z}^{(i)}), \tag{5}$$

where $\mathbf{I}$ is the identity matrix. Since all the variables are in k-space, and $\mathbf{D}$ is a diagonal matrix, the solution can be simplified in a coordinate-wise manner, avoiding a large matrix inversion. For the j^{th} element of $\mathbf{x}^{(i)}$, we have:

$$x_j^{(i)} = \begin{cases} \frac{x_j^{(0)}+\beta_1 u_j^{(i)}+\beta_2 z_j^{(i)}}{1+\beta_1+\beta_2}, & \text{if } j \in \Omega \\ \frac{\beta_1 u_j^{(i)}+\beta_2 z_j^{(i)}}{\beta_1+\beta_2}, & \text{if } j \notin \Omega \end{cases} \tag{6}$$

where Ω defines the indices of acquired elements.

The proposed RNN architecture for solving (2) will then be trained end-to-end using scan-specific k-space data. All the relevant parameters for the CNNs implementing the self-consistency rule $\mathbf{G}(\cdot)$, and the regularizer $\mathcal{R}(\cdot)$, as well as the β_1, β_2 for data-consistency will be learnt during training, and applied during reconstruction. Since neural networks are to learn the self-consistency and regularization terms in this setting, a recurrent neural network (RNN) architecture with a fixed number of iterations needs to be designed to implement the iterative updating scheme of optimization.

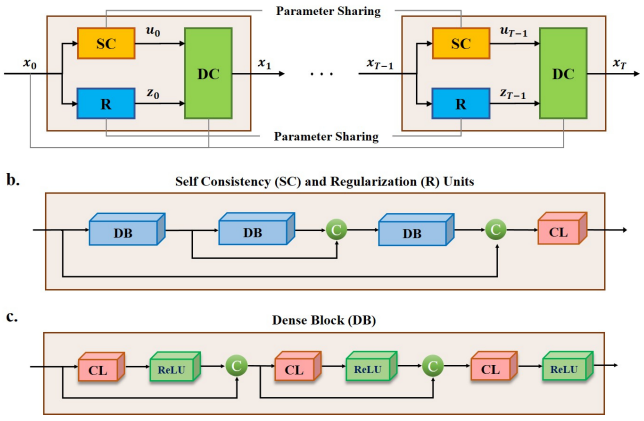

Fig. 1: (a) The recurrent network architecture of regularized sRAKI-RNN unrolled for T iterations to simultaneously apply self-consistency (SC), regularization (R) and data consistency (DC) and perform the iterative reconstruction. (b) A single SC and R unit with 3 dense blocks (DB), a single convolutional layer (CL) at the output, along with two skip connections to facilitate information flow through network. (c) A closer view of the DB, with each CL being followed by a ReLU activation function.

2.2. Implementation Details

The RNN in **Fig. 1** was unrolled for 5 iterations. As detailed in the sub-problems (4a)-(4c), each iteration consists of parallel application of the self-consistency (SC) and regularization (R) units, followed by a data-consistency unit (DC) that combines the initial elements with estimated values to yield the end estimation of the corresponding iteration. SC and DC units are implemented in k-space domain, while the regularization unit first projects the data to the image domain using a non-trainable SENSE-1 operator and then project back the output of the regularizer to k-space using the coil sensitivites. The coil sensitivities are estimated prior to training from the ACS data. Both self-consistency and regularization units share a densely connected convolutional neural network design similar to sRAKI-RNN in [16] with a growth factor of 8 channels and a kernel size of 3×3.

In contrast to our previous works on sRAKI [14, 16], where the networks were trained on ACS data only via retrospective random undesampling, the proposed regularized sRAKI-RNN needs to be trained on the full k-space to avoid regularizers from introducing blurring artifacts associated with low-resolution data. To this end, we utilized a recent self-supervised training method, called SSDU [21, 22]. For a given undersampling pattern, all acquired elements were retrospectively further undersampled by 50%, which were then used to estimate the elements that were removed from the undersampling. We note that since this is a post-processing step during training, there are no physical constraints (e.g. full-sampling along readout) to picking which elements can be used to estimate the remaining ones. The network was trained by minimizing an MSE loss function using Adam op-

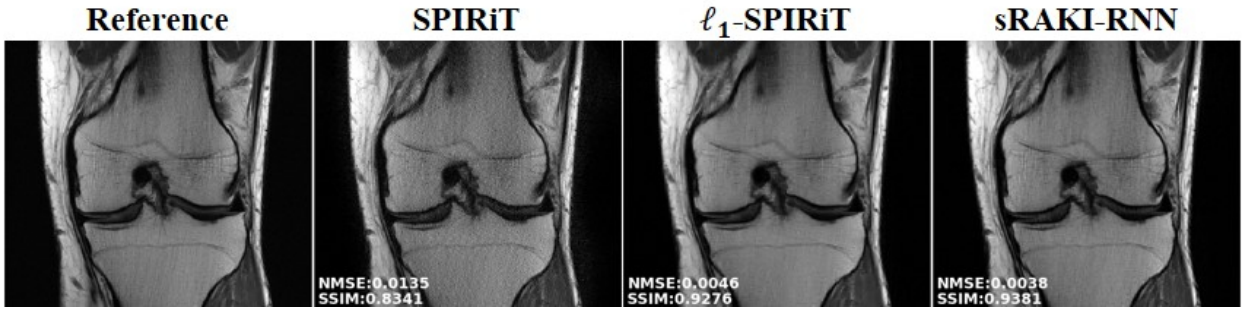

Fig. 2: A proton-density knee dataset from the NYU FastMRI database, retrospectively undersampled using a random variable density pattern at rate 4, and reconstructed using SPIRiT, ℓ_1-SPIRiT and sRAKI-RNN. sRAKI-RNN yields the best performance in terms of reconstruction noise, reduction of blurring artifacts and quantitative metrics.

timizer with a learning rate of 0.01 and 1000 epochs. k-space was normalized to the maximum absolute value of 1. Real and imaginary components were concatenated for processing, resulting in $2n_c$ input and output channels. SPIRiT and ℓ_1-SPIRiT were also implemented for comparison.

2.3. Imaging Experiments

A coronal proton density (PD) knee MRI slice acquired with a 15-channel coil from the NYU fastMRI database was used for reconstruction in a scan-specific manner. A central slice from one subject was selected. The oversampling along readout was removed for a matrix size of 320×368. All data were retrospectively undersampled with a random variable density pattern at an acceleration rate of 4 after keeping 24 ACS lines in the center. The reference image was used to quantitatively assess the reconstructed images according to normalized mean square error (NMSE) and structural similarity index (SSIM) metrics.The experiments were repeated for another coronal PD slice with fat saturation (PDFS).

3. RESULTS

Fig. 2 depicts a coronal PD slice from the NYU fastMRI knee dataset reconstructed using SPIRiT, ℓ_1-SPIRiT and sRAKI-RNN. Reconstruction noise is visibly present in the SPIRiT image, while both ℓ_1-SPIRiT and sRAKI-RNN reduce the noise as expected due to regularization. sRAKI-RNN yields the best results among these techniques in terms of both noise, blurring artifacts and quantitative metrics.

Fig. 3 shows a coronal PDFS slice from the NYU fastMRI knee dataset, reconstructed using the three techniques. Similar to previous results, ℓ_1-SPIRiT and sRAKI-RNN reduce reconstruction noise compared to SPIRiT. Furthermore, sRAKI-RNN leads to improved quantitative results over SPIRiT and ℓ_1-SPIRiT for both data.

4. DISCUSSION

We proposed a method for database-free accelerated MRI reconstruction using recurrent neural network architectures that are trained end-to-end for arbitrary undersampling patterns. sRAKI-RNN used both self-consistency in k-space and regularization in image domain for improved reconstruction. The results indicate that the proposed technique is robust to reconstruction noise amplification and also successfully removes aliasing artifacts. In contrast to compressed sensing, in which both the regularizer and its parameters need to be explicitly specified before reconstruction, sRAKI-RNN learns both of these from the scan data.The way sRAKI-RNN is imple-

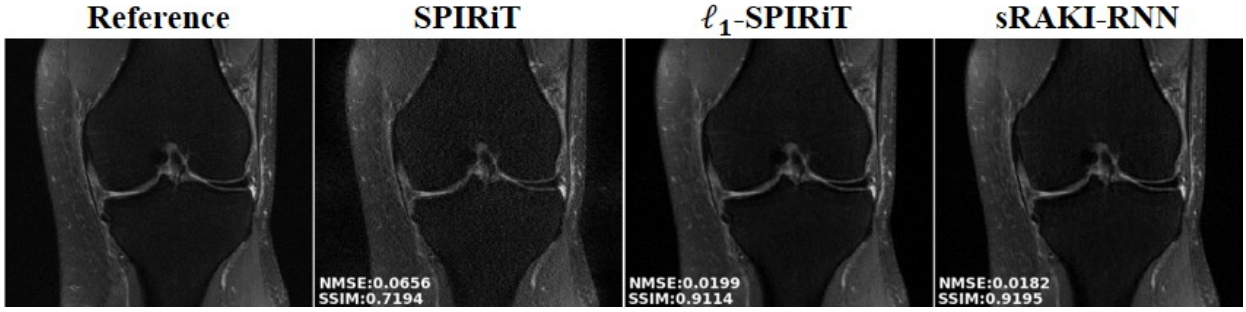

Fig. 3: A proton-density fat-saturated knee dataset from the NYU FastMRI database, retrospectively undersampled using a random variable density pattern at rate 4, and reconstructed using SPIRiT, ℓ_1-SPIRiT and sRAKI-RNN. Both ℓ_1-SPIRiT and sRAKI-RNN reduce reconstruction noise compared to SPIRiT, but sRAKI-RNN outperforms ℓ_1-SPIRiT quantitatively.

mented allows training and reconstruction without requiring fully-sampled data in a scan-specific manner. This is especially important for applications, such as perfusion cardiac MRI where one cannot acquire fully-sampled high-resolution data due to physiological constraints or whole-heart coronary MRI where a fully-sampled scan would be prohibitively long.

5. CONCLUSION

We have proposed an accelerated MRI reconstruction technique using recurrent neural networks that is robust to reconstruction noise amplification. This technique is database-free and the networks are trained individually for each scan.

Acknowledgments

This work was supported by NIH U01EB025144, P41EB027061; NSF CAREER CCF-1651825. Knee MRI data were obtained from the NYU fastMRI initiative database [23]. NYU fastMRI database was acquired with the relevant institutional review board approvals as detailed in [23]. A listing of NYU fastMRI investigators, subject to updates, can be found at `fastmri.med.nyu.edu`.

References

[1] S. Wang, Z. Su, et al., "Accelerating magnetic resonance imaging via deep learning," in *Proc IEEE ISBI*, 2016, pp. 514–517.

[2] K. Kwon, D. Kim, and H. Park, "A parallel MR imaging method using multilayer perceptron," *Medical Physics*, vol. 44, no. 12, pp. 6209–6224, 2017.

[3] J. Schlemper, J. Caballero, et al., "A deep cascade of convolutional neural networks for dynamic MR image reconstruction," *IEEE Trans Med Imaging*, vol. 37, no. 2, pp. 491–503, 2017.

[4] K. Hammernik, T. Klatzer, et al., "Learning a variational network for reconstruction of accelerated MRI data," *Magn Reson Med*, vol. 79, pp. 3055–3071, 2018.

[5] D. Lee, J. Yoo, S. Tak, and J. C. Ye, "Deep residual learning for accelerated MRI using magnitude and phase networks," *IEEE Trans Biomed Eng*, vol. 65, no. 9, pp. 1985–1995, 2018.

[6] M. Akçakaya, S. Moeller, S. Weingärtner, and K. Uğurbil, "Scan-specific robust artificial-neural-networks for k-space interpolation (RAKI) reconstruction: Database-free deep learning for fast imaging," *Magn Reson Med*, vol. 81, no. 1, pp. 439–453, 2019.

[7] H. K. Aggarwal, M. P. Mani, and M. Jacob, "Modl: Model-based deep learning architecture for inverse problems," *IEEE Trans Med Imaging*, vol. 38, no. 2, pp. 394–405, 2018.

[8] Y. Han, L. Sunwoo, and J. C. Ye, "k-space deep learning for accelerated MRI," *IEEE Trans Med Imaging*, 2019.

[9] S. H. Dar and T. Çukur, "Transfer learning for reconstruction of accelerated MRI acquisitions via neural networks," Paris, France, 2018, Proc ISMRM.

[10] K. P. Pruessmann, M. Weiger, M. B. Scheidegger, and P. Boesiger, "SENSE: sensitivity encoding for fast MRI," *Magn Reson Med*, vol. 42, pp. 952–962, 1999.

[11] M. Lustig, D. Donoho, and J. Pauly, "Sparse MRI: The application of compressed sensing for rapid MR imaging," *Magn Reson Med*, vol. 58, pp. 1182–1195, 2007.

[12] Y. C. Eldar, A. O. Hero III, et al., "Challenges and open problems in signal processing: Panel discussion summary from ICASSP 2017," *IEEE Signal Processing Magazine*, vol. 34, pp. 8–23, 2017.

[13] M. Akçakaya, T. A. Basha, et al., "Accelerated isotropic sub-millimeter whole-heart coronary MRI: compressed sensing versus parallel imaging," *Magn Reson Med*, vol. 71, no. 2, pp. 815–822, 2014.

[14] S. A. H. Hosseini, S. Moeller, et al., "Accelerated coronary MRI using 3D SPIRiT-RAKI with sparsity regularization," in *Proc. IEEE ISBI*, 2019, pp. 1692–1695.

[15] S. A. H. Hosseini, C. Zhang, et al., "Accelerated coronary MRI with sRAKI: A database-free self-consistent neural network k-space reconstruction for arbitrary undersampling," *arXiv preprint arXiv:1907.08137*, 2019.

[16] S. A. H. Hosseini, C. Zhang, et al., "sRAKI-RNN: accelerated MRI with scan-specific recurrent neural networks using densely connected blocks," in *SPIE Wavelets and Sparsity XVIII*, 2019, p. 111381B.

[17] C. Qin, J. Schlemper, et al., "Convolutional recurrent neural networks for dynamic MR image reconstruction," *IEEE Trans Med Imaging*, vol. 38, pp. 280–290, 2018.

[18] T. Kim, P. Garg, and J. Haldar, "LORAKI: Reconstruction of undersampled k-space data using scan-specific autocalibrated recurrent neural networks," in *Proc. Int. Soc. Magn. Reson. Med*, 2019, p. 4647.

[19] M. Lustig and J. M. Pauly, "SPIRiT: Iterative self–consistent parallel imaging reconstruction for arbitrary k-space," *Magn Reson Med*, vol. 64, pp. 457–471, 2010.

[20] M. V. Afonso, J. M. Bioucas-Dias, and M. A. Figueiredo, "Fast image recovery using variable splitting and constrained optimization," *IEEE Trans Image Proc*, vol. 19, pp. 2345–2356, 2010.

[21] B. Yaman, S. A. H. Hosseini, et al., "Self-supervised physics-based deep learning MRI reconstruction without fully-sampled data," *Proc IEEE ISBI*, 2020.

[22] B. Yaman, S. A. H. Hosseini, et al., "Self-supervised learning of physics-guided reconstruction neural networks without fully-sampled reference data," *preprint arXiv:1912.07669*, 2019.

[23] J. Zbontar, F. Knoll, et al., "fastMRI: An open dataset and benchmarks for accelerated MRI," *arXiv preprint arXiv:1811.08839*, 2018.